Accepted Manuscript

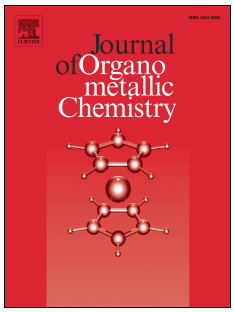

Synthesis, structure and anticancer activity of (η^6-benzene) ruthenium(II) complexes containing aroylhydrazone ligands

Nanjan Mohan, Subramanian Muthumari, Rengan Ramesh

PII: S0022-328X(16)30033-X

DOI: 10.1016/j.jorganchem.2016.01.033

Reference: JOM 19384

To appear in: *Journal of Organometallic Chemistry*

Received Date: 24 November 2015

Revised Date: 21 January 2016

Accepted Date: 28 January 2016

Please cite this article as: N. Mohan, S. Muthumari, R. Ramesh, Synthesis, structure and anticancer activity of (η^6-benzene) ruthenium(II) complexes containing aroylhydrazone ligands, *Journal of Organometallic Chemistry* (2016), doi: 10.1016/j.jorganchem.2016.01.033.

New (η^6-benzene) ruthenium(II) complexes containing aroylhydrazone ligands were synthesized and characterized. The single crystal X- ray analysis of the complex **4** reveals a typical three leg piano stool structure. Complexes are more potent against MCF-7 cells than cisplatin. Fluorescence staining methods confirm apoptosis induced cell death.

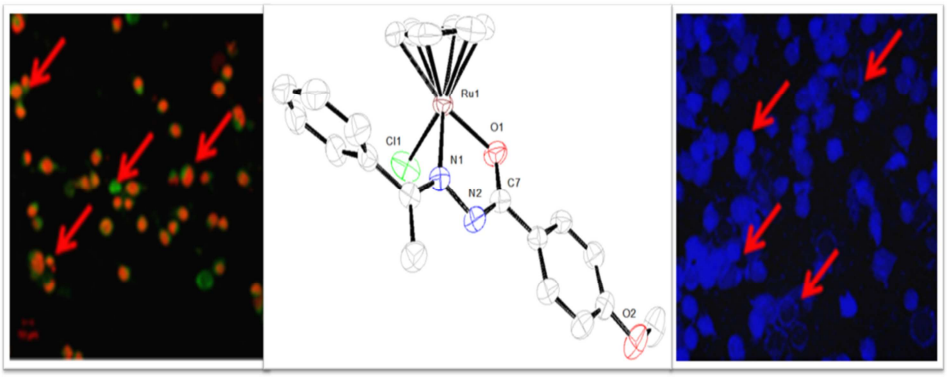

Synthesis, structure and anticancer activity of (η^6-benzene) ruthenium(II) complexes containing aroylhydrazone ligands

Nanjan Mohan, Subramanian Muthumari and Rengan Ramesh*

School of Chemistry, Bharathidasan University, Tiruchirappalli 620 024, Tamil Nadu, India

A B S T R A C T

New benzene ruthenium(II) aroylhydrazone complexes of general molecular formula [Ru(η^6-C_6H_6)Cl(L)] (where L = aroylhydrazone ligand) have been synthesized from the reaction of the precursor [Ru(η^6- C_6H_6)(μ-Cl)Cl]$_2$ and aroylhydrazone ligands. The composition of the complexes has been accomplished by elemental analysis and spectral methods (FT-IR, UV-Vis, ^{1}HNMR). The molecular structure of complex **4** has been established by single-crystal X-ray structure analysis shows that the aroylhydrazone ligands are coordinated to ruthenium as a bidentate N, O donor and a typical piano stool geometry was observed around ruthenium(II) metal center. All the complexes exhibit two consecutive irreversible oxidations in the potential range +0.74 to +1.17 V (Ru^{II}/Ru^{III};Ru^{III}/Ru^{IV}) Vs calomel electrode. Further, *in vitro* anticancer activity of complexes 1-4 on human breast cancer cell line (MCF-7), human cervical cancer cell line (HeLa) and non-cancerous NIH-3T3 cell line exhibit moderate to excellent cytotoxic activity. It is also evident from IC_{50} values that the complexes are more potent against MCF-7 cells than cisplatin. The superior activity of the complex **4** assumes that presence of electron donating methoxy substituent which makes the ring more reactive. Further, the morphological changes during cell death were investigated by Acridine Orange-Ethidium Bromide (AO–EB) and DAPI staining techniques, which confirm the complex **4** induces cell death only through apoptosis.

Keywords:

Aroylhydrazone, Benzene ruthenium(II) complex; Molecular structure; Redox behaviour; Cytotoxicity; Apoptosis

* Corresponding author. Tel.: +91 431 2407053; fax: +91 431 2407045.
E-mail address: ramesh_bdu@yahoo.com (R. Ramesh).

1. Introduction

The pioneering work on the anticancer properties of cisplatin by Rosenberg in 1965 [1] has successfully resulted in using it as an effective drug against cancer for the past few decades. However, this drug shows resistance, high toxicity and other side effects [2, 3]. For this reason ruthenium based drugs have been thought of as an attractive alternative due to their fewer side effects, higher activity [4] and their similarity to iron in binding properties [5]. In addition, most of the ruthenium complexes interact with DNA *in vitro* and display binding modes and better activity when compared to those of platinum based drugs. In particular two ruthenium(III)-based drugs, KP1019 and NAMIA have already entered into clinical trials [6-8], but differ considerably from cisplatin in their *in vivo* behaviour.

Half-sandwich arene ruthenium(II) compounds have been the subject of intense research in recent years because of their lipophilic and hydrophilic properties [9,10]. In addition, all these complexes adopt a typical three-legged piano stool conformation, where the arene ligand forms the seat and the chelating ligand along with auxiliary ligand are the legs of the piano stool. It is to be considered that arene Ru(II) complexes often possess good aqueous solubility along with satisfactory lipophilicity needed to cross the cell membrane. Moreover, the coordinated arene stabilizes ruthenium in the +2 oxidation state and different types of substituent can be modified to tune the properties of the arene-ruthenium complexes. The ligand exchange kinetics of Pt(II) and Ru(II) complexes are very similar in aqueous solution, pivotal for anticancer activity [11]. The mechanism of cytotoxic involves the hydrolysis of the Ru-X bond giving rise to the active targeting species [12]. However, arene ruthenium complexes of the type [Ru(η^6-arene)(PTA)Cl_2] (PTA = 1,3,5-triaza-7-phosphaadamantane) [13], (η^6-arene)$RuCl_2$(imidazole) [14], (η^6-arene)$RuCl_2$(DMSO) [15], [Ru(η^6-arene)(YZ)Cl][PF_6] [16] (YZ = chelating diamine) as well as dinuclear compounds [17], and the tri [18] and tetranuclear clusters [19] such as $[H_3Ru_3(\eta^6–C_6H_6)(\eta^6–C_6Me_6)_2O]^+$ and $[H_4Ru_4(\eta^6–C_6H_6)_4]^{2+}$ have been studied *in vitro* and in some cases *in vivo* for their antitumor activity. Recent studies have shown that metal complexes bind to the primary target DNA as well as strongly interact with proteins [9, 13b, 20 &21]. Therefore, advancement of the anticancer agents targeting both DNA and proteins are most sought after [13b, 20-22].

Aroylhydrazones are versatile ligands exhibiting amide-imidol tautomerism **(Scheme 1)** and display interesting coordination modes in metal complexes. Depending on the acidity, the reaction conditions and the nature of the metal ion, these ligands coordinate to the metal ion via the azomethine nitrogen either in the neutral amide form or in the monobasic

imidolate form, as bidentate N, O donor ligands forming five-membered chelate rings with the metal [23]. Various studies have also shown that the azomethine group having a lone pair of electrons in either a p or sp^2 hybridized orbital on trigonally hybridized nitrogen has considerable biological importance [24]. Though several hydrazone complexes of Cu(II), Ni(II), Pd(II), Pt(II), Co(II), V(V) and Ru(II) [25-31] have been studied, the biological applications of arene ruthenium(II) complexes with hydrazone ligands are not well explored.

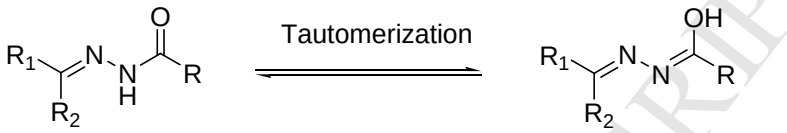

Scheme 1. Amide and imidol forms of hydrazone.

With the objective of promoting the applications of ruthenium(II) hydrazone complexes, we report here the synthesis and spectral characterization of a series of benzene ruthenium(II) complexes containing aroylhydrazone ligands. The molecular structure of one of the complexes was determined by single crystal X-ray diffraction. The redox property of the complexes was examined by cyclic voltammetry. *In vitro* anticancer activity of these complexes against human cancer cell lines and the effect of the substituents present on the ligand on the above said properties were described. Further, the mechanism of cancer cell death was also investigated by AO–EB and DAPI staining techniques.

2. Results and discussion

The aroylhydrazone ligand derivatives were conveniently prepared in an excellent yield by the condensation of acetophenone with substituted benzhydrazides in an equimolar ratio. These ligands were allowed to react with the ruthenium(II) precursor, $[Ru(\eta^6\text{-}C_6H_6)(\mu\text{-}Cl)Cl]_2$ in a 2:1 molar ratio in the presence of triethylamine as the base and the new complexes of the general formula, $[Ru(\eta^6\text{-}C_6H_6)Cl(L)]$ **(Scheme 2)** were obtained in reasonable yields. The addition of triethylamine to the reaction mixture was used to remove a proton from the imidol oxygen and to facilitate the coordination of the imidolate oxygen to the ruthenium(II) ion. The synthesised benzene ruthenium(II) complexes are soluble in solvent such as benzene, toluene, chloroform, dichloromethane, acetonitrile, dimethyl

formamide, dimethyl sulphoxide as well as in water. The analytical data of all the benzene ruthenium(II) complexes are in good agreement with the molecular structures proposed.

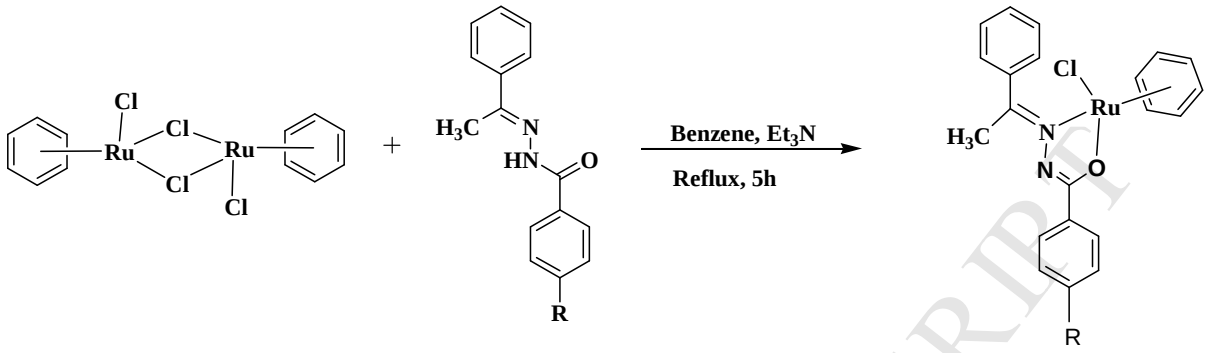

R = -H (L1), -Cl (L2), Br (L3), -OCH_3 (L4)

Scheme 2. Synthesis of benzene ruthenium(II) aroylhydrazone complexes.

2.1. Spectral characterization

The FT-IR spectra of the ligands showed a medium to strong band in the region 3180-3196 cm^{-1} which is characteristic of the $\nu_{(N-H)}$ functional groups respectively. The free ligand also display $\nu_{(C=N)}$ 1539-1576 cm^{-1} and $\nu_{(C=O)}$ absorptions in the region 1610-1653 cm^{-1}. The bands due to N-H and C=O stretching vibrations are also not observed in the complexes indicating that the ligand undergo tautomerisation and subsequent coordination of the imidolate oxygen to the ruthenium(II) ion. This is further supported by the appearance of new bands in the region 1524-1530 cm^{-1} which may be attributed to the C=N-N=C fragments [32] and disappearance of $\nu_{(C=O)}$and appearance of $\nu_{(N=C-O)}$ and $\nu_{(C-O)}$ in the region 1474-1486 and 1369-1396 cm^{-1} respectively [33], in all the metal (II) complexes therefore ascertain the coordination mode of the aroylhydrazone ligand to ruthenium(II) ion via the azomethine nitrogen and the imidolate oxygen. (Fig. S1-S4, Supporting information)

The electronic spectra of all the benzene ruthenium(II) complexes were recorded in dry chloroform solution in the range 200-800 nm. All the complexes display three intense absorptions in the region 400-230 nm. The absorption spectra of the benzene ruthenium(II) aroylhydrazone complexes exhibited very intense band around 266-288 nm and 241-244 nm are assigned to ligand-centered (LC) π-π^* and n-π^* transitions respectively. The lowest energy absorption bands in the electronic spectra of the complexes in the visible region 315-326 nm are ascribed to metal to ligand charge transfer MLCT transitions. Based on the

pattern of the electronic spectra of all the complexes an octahedral environment around the ruthenium(II) ion has been proposed similar to that of the other octahedral ruthenium(II) complexes.

2.2. ^{1}H NMR spectra

The bonding arrangement is further supported by ^{1}H NMR spectra (Table 1). The ^{1}H NMR spectra of all the complexes were recorded in $CDCl_3$. The multiplets observed in the region around δ 6.8-8.1 ppm in all the complexes have been assigned to the aromatic protons of the aroylhydrazone ligand. The singlet in the region δ 2.8 ppm is due to methyl protons nearer to coordinated azomethine group. In addition, peaks around δ 8.9-9.2 ppm for –NH disappeared in all the complexes due to enolisation followed by deprotonation on imidole oxygen indicating that the ruthenium is coordinated through imidolate oxygen. The singlet around δ 3.8 ppm is due to methoxy protons in the complex **4** and singlet in the region δ 5.0 ppm corresponding to the protons of the arene ligand. (Fig. S5-S8, Supporting information)

Table 1

^{1}H NMR data of benzene ruthenium(II) aroylhydrazone complexes

complexes	^{1}H NMR data δ/ppm			
	Ar-H	C_6H_6	$-CH_3$	$-OCH_3$
1	7.2–8.1	5.0	2.8	--
2	7.2–8.0	5.0	2.8	--
3	7.2–8.0	5.0	2.8	--
4	6.8–8.1	5.0	2.8	3.8

2.3. X-ray structure determination

The molecular structure of one of the benzene ruthenium(II) complexes [Ru(η^6-C_6H_6)Cl(L4)] **4** has been confirmed by a single – crystal X-ray diffraction analysis in order to confirm the coordination mode of the ligand and geometry of the complex. The single crystals of the complex **4** were obtained from slow evaporation of dichloromethane-petroleum ether solution at room temperature. The ORTEP view of complex **4** is shown in Fig. 1. The summary of the data collection and refinement parameters are given in (Table 2)

and selected bond lengths and angles are given in (Table 3). The complex **4** crystallize in the monoclinic space group P2(1)/n. The benzene ligand is bonded to the ruthenium atom in η^6 fashion with ruthenium centroid. The complex adopt a typical three-legged piano stool conformation with N, O and Cl atoms as the legs and evident by the nearly 90^0bond angles for N(1)-Ru(1)-Cl(1) 84.64(6) and O(1)-Ru(1)-Cl(1) 85.81(7). The aroylhydrazone ligand bind to the metal center at N and O forming the five membered chelate ring with bite angle 76.64(8) O-Ru-N and bond length of Ru-N and Ru-O are 2.107(2) and 2.0420(18) respectively. The Ru-Cl bond length is found to be 2.3907(8). The ruthenium atom is π bonded to the benzene ring with an average Ru–C distance of 2.170(3) Å, whereas average distance of ruthenium to the chelating nitrogen and oxygen atoms is 2.074 Å. The average C–C bond length in the benzene ring is 1.391 Å with alternating short and long bonds. As all the four benzene ruthenium(II) complexes show similar spectral properties, the other three complexes are considered to have similar structure as that of complex **4**.

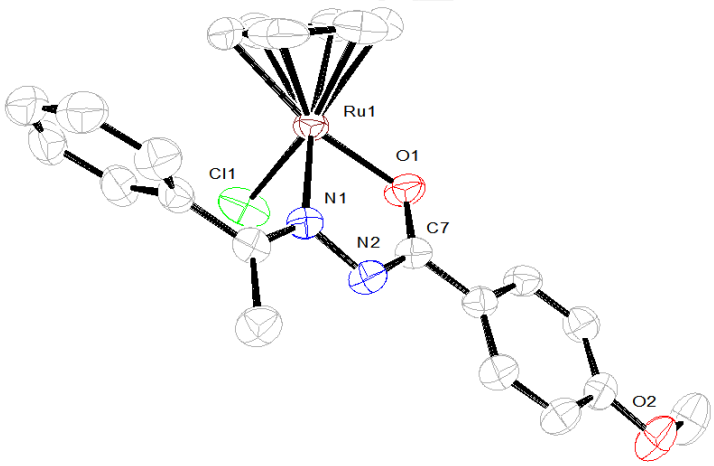

Fig. 1. ORTEP diagram of the complex [Ru(η^6-C_6H_6)Cl(L4)] (**4**), showing 50% probability level.

Table 2

Crystal data and structure refinement for complex **4**

Compound	4
Formula	$C_{22}H_{21}ClN_2O_2Ru$
Formula weight	481.93
Temperature	296(2) K
Wavelength	0.71073 A
Crystal system, space group	Monoclinic, P21/n
Unit cell dimensions	a = 10.0868(7) Å alpha = 90 deg. b = 19.0613(14) Å beta = 98.585(3) deg. c = 10.4898(7) Å gamma = 90 deg.
Volume	1994.2(2) $Å^3$
Z, Calculated density	4, 1.605 Mg/m^3
Absorption coefficient	0.940 mm^{-1}
F(000)	976
Crystal size	0.35 x 0.30 x 0.30 mm
Theta range for data collection	2.24 to 28.55 deg.
Limiting indices	$-13 \le h \le 10$, $-25 \le k \le 25$, $-13 \le l \le 12$
Reflections collected / unique	16583 / 4908 [R(int) = 0.0217]
Completeness to theta = 28.55	96.7 %
Absorption correction	Semi-empirical from equivalents
Max. and min. transmission	0.7656 and 0.7343
Refinement method	Full-matrix least-squares on F^2
Data / restraints / parameters	4908 / 0 / 255
Goodness-of-fit on F^2	1.097
Final R indices [I>2sigma(I)]	R1 = 0.0306, wR2 = 0.0832
R indices (all data)	R1 = 0.0411, wR2 = 0.0968
Largest diff. peak and hole	0.480 and -0.600 $e.Å^{-3}$

Table 3

Selected bond lengths (Å) and angles (^{0}) for complex **4**

Bond lengths (Å)		Bond angles (^{0})	
N(1)-N(2)	1.402(3)	N(2)-N(1)-Ru(1)	113.69(14)
N(1)-Ru(1)	2.107(2)	C(7)-N(2)-N(1)	111.10(2)
O(1)-Ru(1)	2.042(18)	C(7)-O(1)-Ru(1)	113.12(16)
Cl(1)-Ru(1)	2.390(8)	O(1)-Ru(1)-N(1)	76.64(8)
C(7)-O(1)	1.288(3)	O(1)-Ru(1)-Cl(1)	85.81(7)
C(7)-N(2)	1.309(3)	N(1)-Ru(1)-Cl(1)	84.64(6)

ESD in parenthesis.

2.4. Electrochemical property

Electrochemical study was carried out for all the free ligands and the benzene ruthenium(II) aroylhydrazone complexes in degassed acetonitrile at room temperature in the potential range of 0 to +1.5. The supporting electrolyte used was 0.05 M tetrabutylammonium perchlorate (TBAP) and the concentration of the complex was 10^{-3}M. The resulting data are summarised in (Table4). All the complexes exhibit two consecutive one electron irreversible oxidations in the potential range of 0.74 to +1.17 V at the scan rate of 100 mV $s^{-1}$with reference to saturated calomel electrode (Fig. S9-S12, Supporting information). The comparison of its current height with that of the standard ferrocene/ferrocenium couple under identical conditions reveals the one electron transfer process. The first oxidative response with Epa in the range +0.74 to +0.79 V is assigned to $Ru^{II} \rightarrow Ru^{III}$ oxidation whereas the second one in the range +1.12 to +1.17 V is assigned to $Ru^{III} \rightarrow Ru^{IV}$ oxidation. These potentials are comparable with $Ru^{II} \rightarrow Ru^{III}$ and $Ru^{III} \rightarrow Ru^{IV}$ oxidation potential of other mononuclear ruthenium complexes [34, 35]. In addition, irreversibility observed for the oxidative responses may be due to the fast dissociation of chloride ligand from ruthenium(II) complexes [36]. It is worth noting that correlation between the Epa values and IC_{50} values has been observed for arene ruthenium compounds with anticancer properties [37]. The values between +0.74 and +0.79 V, the Ru^{II}/Ru^{III} redox potentials for complex 1–4 are lower than those for the more cytotoxic complexes [(η^6-arene)$RuCl_2(NC_5H_4OOCC_5H_4FeC_5H_5)$], the Epa values ranging from +0.91 to +1.00 V [38], but significantly higher than the Ru^{II}/Ru^{III} redox potentials for the complex [(η^6-arene)-$Ru(SC_5H_4NH)_3]^{2+}$, the Epa values ranging from +0.58 and +0.67 V [37].

Table 4

Electrochemical data of benzene ruthenium(II) aroylhydrazone complexes

Complexes	Ru^{III} / $Ru^{II}Ru^{IV}$ / Ru^{III}	
	Epa (V)	Epa (V)
1	+0.76	+1.14
2	+0.78	+1.16
3	+0.79	+1.17
4	+0.74	+1.12

Solvent = Acetonitrile; [Complex] = $1x10^{-3}$M; Supporting electrolyte [Bu_4N] (ClO_4) (0.05 M); Scan rate: $100mVs^{-1}$; All potentials referenced to SCE; Epa = anodic peak potential.

2.5. *In vitro* cytotoxic activity

The potential of the complexes to inhibit cancer cell growth was evaluated using the MTT assay. The *in vitro* cytotoxicity of the metallic precursors, ligand and benzene ruthenium(II) complexes **1-4,** was evaluated against human breast cancer (MCF-7) cells, human cervix carcinoma (HeLa) cells and non-cancerous NIH-3T3 mouse embryonic fibroblasts cell lines using MTT assay after **24** hours of inhibition, which measures mitochondrial dehydrogenase activity as an indication of cell viability. For comparison, the cytotoxicity of known anti-cancer drug cisplatin has also assessed against all the above cell lines. The results were analysed by means of cell inhibition of cancer cell growth at the 50% level expressed as IC_{50} values and the values of the four benzene ruthenium(II) complexes **1-4** are listed in (Table 5). It is to be noted that the precursor and the ligand did not show any inhibition of the cell growth even up to 100 μM and clearly indicates chelation of the ligand with metal ion is responsible for the observed cytotoxicity properties of the complexes. All the complexes have moderate to excellent cytotoxic activity against MCF-7, HeLa and NIH-3T3 cell line used. It is found that all the complexes are more potent against MCF-7 cells as compared to other cell lines. Among them, complex **4** exhibit excellent IC_{50} against MCF cell lines. The superior activity of the complex **4** assumes that presence of electron donating methoxy substituent which makes the ring more reactive and thereby increases of the lipophilic character of the metal complex which favours its permeation through the lipid layer of the cell membrane [39]. Hence, the cytotoxicity increases in the order H < Br < Cl < OCH_3. It should be noted that the observed IC_{50} values of the reported complexes are considerably better against MCF-7 cell line than those characteristic of cisplatin. Further, the IC_{50} values of the complexes are much better than those previously reported arene ruthenium(II)

complexes [40]. The excellent cytotoxic activity observed for **4** against the tested cell lines may be due to better cellular uptake inside the cells which is evident by fluorescence images.

Table 5

The cytotoxic activity of benzene ruthenium(II) aroylhydrazone complexes

Complexes	[a]IC_{50} values (μM)		
	MCF-7	HeLa	NIH-3T3
1	15.8 ± 0.4	48.7 ± 0.9	192.4 ± 2.1
2	12.8 ± 0.7	38.4 ± 0.9	178.7 ± 1.0
3	13.5 ± 0.3	41.5 ± 0.6	152.6 ± 1.9
4	10.9 ± 0.3	34.3 ± 1.3	182.8 ± 0.9
Cisplatin	15.2 ± 0.5	11.7 ± 0.7	240.9 ± 1.9

[a]IC_{50} = concentration of the drug required to inhibit growth of 50% of the cancer cells (μM).

2.6. Morphological changes in AO/EB and DAPI fluorescence study

Cell apoptosis is an important phenomenon responsible for destroying undesirable cells during the development and homeostasis of cellular organisms [41]. As such, the ability to kill tumor cells through the induction of apoptosis has been used as a marker for the identification of antitumor drugs [42]. Cells undergoing apoptosis are characterized by morphological and biochemical changes including cell shrinkage, chromatin condensation and DNA fragmentation [43]. Apoptotic cells reveal increased plasma membrane permeability to certain fluorescent dyes, e.g., AO/EB, Hoechst, AO/PI, DAPI etc. In this study, we have carried out AO/EB and DAPI staining methods. To investigate the morphological changes, the most active compound **4** in MCF-7 cells were further studied using Acridine Orange/Ethidium Bromide (AO/EB) staining technique to perceive whether the inhibition is due to apoptotic induction or nonspecific necrosis and the resulting images of the control and treated MCF-7cells are depicted in Fig. 2 and 3. Acridine Orange permeates the intact cell membrane and stains the nuclei green, whereas Ethidium Bromide is excluded from the cells having intact plasma membrane and stains the DNA of dead cells, showing orange fluorescence. Furthermore, in DAPI staining the control cells shows clear intensity but the treated cells with the complex shows strong fluorescence intensity. The cells treated with the complex in the dark did not show any significant nuclear morphological change. The microscopic image Fig. 2 and 3 gives clear evidence of the formation of more apoptotic bodies, characterized by the fragmentation of nuclei with condensed chromatin, upon the treatment of MCF-7 with compound **4**.

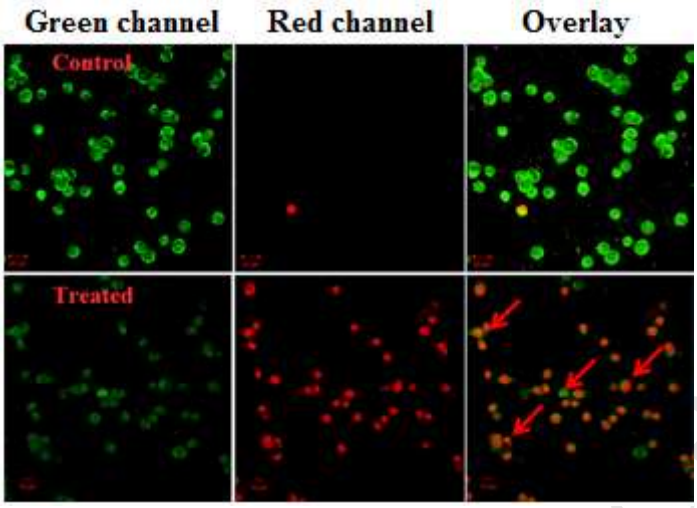

Fig.2. Morphological changes in human breast cancer MCF-7cell treated with compound 4 for 24 h.

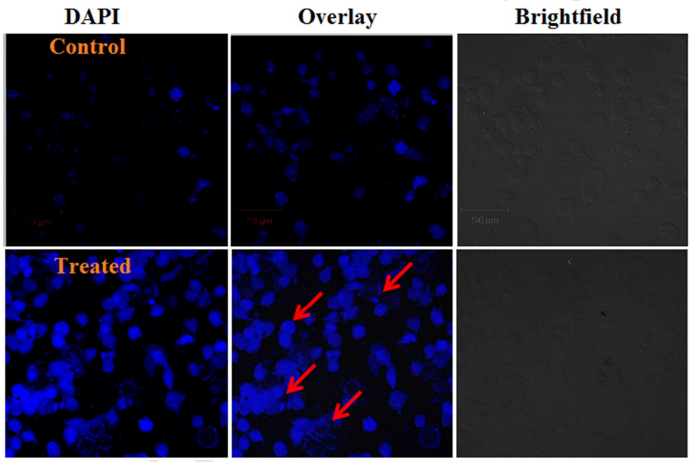

Fig.3. Morphological changes in human breast cancer MCF-7 cell treated with compound 4 for 24 h.

3. Conclusions

A series of benzene ruthenium(II) aroylhydrazone complexes has been synthesised and characterized by analytical and spectroscopic methods. The molecular structure of **4** has been studied by single-crystal X-ray structure analysis indicates that the aroylhydrazone ligands are coordinated to ruthenium as a bidentate N, O donor and a typical piano stool structure was observed around ruthenium(II) metal center. All the complexes (1-4) show moderate to excellent cytotoxic activity against MCF-7 and HeLa cell line used. Particularly the complexes are more active against MCF-7 cells as compared to other cell lines. Among all the complexes, **4** is found to have higher cytotoxicity (10.9 μM against MCF-7 cancer cell

lines). The microscopic images give clear evidence of the formation of more apoptotic bodies, characterized by the fragmentation of nuclei with condensed chromatin, upon the treatment of MCF-7 with compound **4**.

4. Experimental

4.1. Reagents and materials

$RuCl_3.3H_2O$ is commercially available and was used as supplied from Loba chemie Pvt. Ltd. Ketones and benzhydrazide derivatives were purchased from Aldrich and were used as received. The supporting electrolyte, tetrabutylammonium perchlorate (TBAP) was purchased from Aldrich and dried in vacuum prior to use. All other chemicals were obtained from commercial sources and were used as received. The Solvents were distilled following the standard procedures [44] and degassed before use. The precursor $[Ru(\eta^6\text{-}C_6H_6)(\mu\text{-}Cl)Cl]_2$ complex was prepared by reported literature method [45].

The human breast cancer cell line (MCF-7), human cervical cancer cell line (HeLa) and non-cancerous NIH-3T3 mouse embryonic fibroblasts cell line were obtained from the National Center for Cell Science (NCCS), Pune, India.

4.2. Physical measurements

FT-IR spectra were recorded in KBr pellets with JASCO 400 plus spectrometer. The microanalysis of carbon, hydrogen, nitrogen and sulphur were recorded by an analytical function testing Vario EL III CHNS elemental analyser at the Sophisticated Test and Instrumentation Centre (STIC), Cochin University, Kochi. Electronic spectra in chloroform solution were recorded with a CARY 300 Bio UV- visible Varian spectrometer. ^{1}H NMR spectra were recorded on a Bruker 400 MHz instruments using tetramethylsilane (TMS) as an internal reference. Electrochemical measurements were made using a CH Instruments, Inc. Model 600E SN: I1140 Electrochemical Analyser using a glassy carbon working electrode, Pt wire as counter electrode and all the potentials were reference to saturated calomel electrode. Melting points were recorded with a Boetius micro-heating table and are corrected.

4.3. Preparation of aroylhydrazone ligand

A mixture of 4-substituded benzhydrazide (0.01 mmol) and acetophenone (0.01 mmol) in methanol (30 mL) was refluxed for 30 min. The separated solid was filtered and dried in air. Yield**:** 87-91%.

4.4. Synthesis of benzene ruthenium(II) aroylhydrazone complexes

The complexes were prepared using a general procedure in which $[Ru(\eta^6\text{-}C_6H_6)(\mu\text{-}Cl)Cl]_2$ (25mg, 0.04 mmol) with aroylhydrazone ligand (19.4-25.8 mg, 0.08 mmol) in the presence of Et_3N (0.5 mL) in benzene 30 mL. The resulting solution was refluxed for 5h and the progress of the reaction was monitored by TLC. At the end of the reaction the solution was concentrated to about 3 mL and petroleum ether was added whereby solid separated out. The obtained solid was recrystallized from CH_2Cl_2-petroleum ether at room temperature. Yield**:** 70-81%.

4.4.1. [**$Ru(\eta^6\text{-}C_6H_6)(Cl)(L1)$**]

Colour: Brown; Yield: 81%; M.p.: 170 ^{0}C (with decomposition); Anal. Calc. for $C_{21}H_{19}ClN_2ORu$: C, 55.81; H, 4.23; N, 6.19%. Found: C,55.71; H, 4.17; N, 6.25%. IR (KBr, cm^{-1}):1530 $\nu_{(C=N-N=C)}$, 1486 $\nu_{(N=C-O)}$, 1376 $\nu_{(C-O)}$. UV–Vis (CH_3CN, λmax/nm; ε/dm^3 mol^{-1} cm^{-1}): 315(7261), 266(10,825), 243(12,234). ^{1}H NMR (400 MHz, $CDCl_3$) (δ ppm): 7.2–8.1 (m, 10H, aromatic), 5.0(s, 6H), 2.8 (s, 3H, CH_3).

4.4.2. [**$Ru(\eta^6\text{-}C_6H_6)(Cl)(L2)$**]

Colour: Brown; Yield: 76%; M.p.: 165 ^{0}C (with decomposition); Anal. Calc. for $C_{21}H_{18}Cl_2N_2ORu$: C, 51.86; H, 3.73; N, 5.75%. Found: C,51.81; H, 3.77; N, 5.70%. IR (KBr, cm^{-1}):1524 $\nu_{(C=N-N=C)}$, 1482 $\nu_{(N=C-O)}$, 1376 $\nu_{(C-O)}$. UV–Vis (CH_3CN, λmax/nm; ε/dm^3 mol^{-1} cm^{-1}): 320(2494), 267(4293), 242(4817). ^{1}H NMR (400 MHz, $CDCl_3$) (δ ppm): 7.2–8.0 (m, 9H, aromatic), 5.0(s, 6H), 2.8 (s, 3H, CH_3).

4.4.3. [**$Ru(\eta^6\text{-}C_6H_6)(Cl)(L3)$**]

Colour: Brown; Yield: 70%; M.p.: 162 ^{0}C (with decomposition); Anal.Calc. for $C_{21}H_{18}ClN_2BrORu$: C, 47.51; H, 3.41; N, 5.27%. Found: C,47.51; H, 3.47; N, 5.25%. IR (KBr, cm^{-1}

^{1}):1529 $\nu_{(C=N-N=C)}$, 1477 $\nu_{(N=C-O)}$, 1369 $\nu_{(C-O)}$. UV–Vis (CH_3CN, λmax/nm; ε/dm^3 mol^{-1} cm^{-1}): 320(4913), 268(830), 244(8673). ^{1}H NMR (400 MHz, $CDCl_3$) (δ ppm): 7.2–8.0 (m, 9H, aromatic), 5.0(s, 6H), 2.8 (s, 3H, CH_3).

4.4.4. [**Ru(η^6-C_6H_6)(Cl)(L4)]**

Colour: Brown; Yield: 72%; M.p.: 159 ^{0}C (with decomposition); Anal. Calc. for $C_{22}H_{21}ClN_2O_2Ru$: C, 54.82; H, 4.39; N, 5.81%. Found: C,54.88; H, 4.36; N, 5.85%. IR (KBr, cm^{-1}):1525 $\nu_{(C=N-N=C)}$, 1474 $\nu_{(N=C-O)}$, 1396 $\nu_{(C-O)}$. UV–Vis (CH_3CN, λmax/nm; ε/dm^3 mol^{-1} cm^{-1}): 326(4061), 288(5749), 241(6109). ^{1}H NMR (400 MHz, $CDCl_3$) (δ ppm): 6.8–8.1 (m, 9H, aromatic), 5.0(s, 6H), 2.8 (s, 3H, CH_3), 3.8 (s, 3H, OCH_3).

4.5. X-ray crystallography

Single crystal of [Ru(η^6-C_6H_6)Cl(L4)] (4) were grown by slow evaporation of Dichloromethane-Petroleum ether solution at room temperature. A single crystal of suitable size was covered with Paratone oil, mounted on the top of a glass fiber, and transferred to a Bruker AXS Kappa APEX II single crystal X-ray diffractometer using monochromated Mo-Kα radiation (λ=0.71073). Data were collected at 293K. The structure was solved with direct method using SIR-97 [46] and was refined by full matrix least-squares method on F^2 with SHELXL-97[47]. Non-hydrogen atoms were refined with anisotropy thermal parameters. All hydrogen atoms were geometrically fixed and collected to refine using a riding model. Frame integration and data reduction were performed using the Bruker SAINT-Plus (Version 7.06a) software. The multiscan absorption corrections were applied to the data using SADABS software. CCDC reference number is **1064013.**

4.6. *In vitro* cytotoxic activity. maintenance of cell lines

The assays were carried out in monolayer cells were detached with trypsin-ethylenediaminetetraacetic acid (EDTA) to make single cell suspensions and viable cells were counted using a hemocytometer and diluted with medium containing 5% FBS to give final density of $1x10^5$ cells/ml. One hundred microliters per well of cell/well and incubated to allow for cell attachment at 37 °C, 5% CO_2, 95% air and 100% relative humidity. After 24

hours the cells were treated with serial concentrations of the test samples. They were initially dissolved in neat DMSO to prepare the stock (200 µM) and stored frozen prior to use. At the time of drug addition, the frozen concentrate was thawed and an aliquot was diluted to twice the desired final maximum test concentration with serum free medium. Additional three, 10 fold serial dilutions were made to provide a total of four drug concentrations. Aliquots of 100 µL of these different drug dilutions were added to the appropriate wells already containing 100 µL of medium, resulted the required final drug concentrations. Following drug additions the plates were incubated for an additional 24 h at 37 ^{0}C, 5% CO_2, 95% air and 100% relative humidity. The medium containing no samples served as a control and triplicate was maintained for all concentrations.

4.7. Evaluation by MTT assays

MTT is a yellow water soluble tetrazolium salt. A mitochondrial enzyme in living cells, succinate-dehydrogenase, cleaves the tetrazolium ring, converting the MTT to an insoluble purple colour formazan. Therefore, the amount of formazan produced is directly proportional to the number of viable cells after 24 h of plating benzene ruthenium(II) complexes 1-4 were added at various concentration (1 to 100 µM for 24 h, with a final volume in the well of 300 µL) for 24 h to study the dose dependent cytotoxic effect. To each well, 15 µL of MTT (5 mg/mL) in phosphate buffered saline was added to each well and incubated at 37 ^{0}C for 4 h. The medium with MTT was then flicked off and the formed formazan crystals were solubilized in 100 µL of DMSO and then the absorbance at 570 nm was using micro plate reader. Nonlinear regression graph was plotted with the percentage of cell inhibition versus log10 concentration. From this, the IC_{50} value was calculated by using the following formula.

% cell inhibition= 1-Abs (sample)/Abs (control) x100.

4.8. Fluorescent dual staining experiment

Acridine Orange and Ethidium Bromide (AO and EB) staining was performed as follows: the cell suspension of each sample containing 5 x 10^5 cells, was treated with 25 µL of AO and EB solution (1 part of 100 µg mL^{-1} AO and 1 part of µg mL^{-1} EB in PBS) and examined in a laser scanning confocal microscope LSM 710 (Carl Zeiss, Germany) using an UV filter (450–490 nm). Three hundred cells per sample were counted in triplicate for each dose point.

The cells were scored as viable, apoptotic or necrotic as judged by the staining, nuclear morphology and membrane integrity. Morphological changes were also observed and photographed.

4.9. DAPI staining method

DAPI (4', 6'-diamidino−2−phenylindole) staining was done using the following procedure: 5×10^5 cells were treated with the complex 4 (100 μg mL^{-1}) for 24 h in a 6-well culture plate and were fixed with 4% paraformaldehyde followed by permeabilization with 0.1% Triton X-100. Cells were then stained with 50 μg mL^{-1} DAPI for 30 min at room temperature. The cells undergoing apoptosis, represented by the morphological changes of apoptotic nuclei, were observed and imaged from ten eye views at under a laser scanning confocal microscope LSM 710 (Zeiss).

Acknowledgments

One of the authors (N. M) thanks University Grants Commission (UGC), New Delhi, for the award of UGC-RFSMS. We express sincere thanks to DST-FIST, India for the use of Bruker 400 MHz spectrometer at the School of Chemistry, Bharathidasan University, Tiruchirappalli. We also thank the CSIR, New Delhi for Electrochemical Analyser through research project [Ref. No: 02 (0142) /13/EMR-II].

Appendix A. Supplementary material

CCDC 1064013 contains the supplementary crystallographic data for this paper. These data can be obtained free of charge from The Cambridge Crystallographic Data Centre via www.ccdc.cam.ac.uk/data_request/cif.

[1] B.Rosenberg, L. VanCamp, J.E. Trosko, V.H. Mansour, Nature 222 (1969) 385-386.
[2] E. Wong, C.M. Giandomenico, Chem. Rev. 99 (1999) 2451-2466.
[3] M. Galanski, M.A. Jakupec, B.K. Keppler, Curr. Med. Chem. 12 (2005) 2075-2094.
[4] C.S. Allardayce, P.J. Dyson,Platin. Met. Rev. 45 (2001) 62-69.

[5]M. Pongratz, P. Schluga, M.A. Jakupec, V.B. Arion, C.G. Hartinger, G. Allmaier, B.K. Keppler, J.Anal. At. Spectrom.19 (2004) 46-51.

[6] J.M. Rademaker-Lakhai, D. Van Den Bongard, D. Pluim, J.H. Beijnen and J.H.M. Schellens, Clin. Cancer Res.10 (2004) 3717-3727.

[7]C.G. Hartinger, S. Zorbas-Seifried, M.A. Jakupec, B. Kynast, H. Zorbas and B.K. Keppler, J. Inorg. Biochem. 100 (2006) 891-904.

[8] C.G. Hartinger, M.A. Jakupec, S. Zorbas-Seifried, M. Groessl, A. Egger, W. Berger, H. Zorbas, P.J. Dyson and B.K. Keppler, Chem. Biodiversity. 5(2008) 2140-2155.

[9] G. Suss-Fink, Dalton Trans. 39 (2010) 1673-1688.

[10] G. Sava, A. Bergamo, P.J. Dyson, Dalton Trans. 40 (2011) 9069-9075.

[11] J. Reedijk, Platin. Met. Rev. 52 (2008) 2-11.

[12] C. Scolaro, A.B. Chaplin, C.G. Hartinger, A. Bergamo, M. Cocchietto, B.K. Keppler, G. Sava, P.J. Dyson, Dalton Trans. 43 (2007) 5065-5072.

[13] (a) C. Scolaro, T.J. Geldbach, S. Rochat, A. Dorcier, C. Gossens, A. Bergamo, M. Cocchietto, I. Tavernelli, G. Sava, U. Rothlisberger, P.J. Dyson, Organometallics 25 (2006) 756-765;

(b) A. Dorcier, P.J. Dyson, C. Gossens, U. Rothlisberger, R. Scopelliti, I.Tavernelli, Organometallics 24 (2005) 2114-2123;

(c) C.S. Allardyce, P.J. Dyson, D.J. Ellis, S.L. Heath, Chem. Commun. 15 (2001) 1396-1397.

[14] (a) W.H. Ang, A.De Luca, C. Chapuis-Bernasconi, L. Juillerat-Jeanneret, M. Lo Bello, P.J. Dyson, Chem. Med. Chem. 2 (2007) 1799-1806;

(b) C.A. Vock, W.H. Ang, C. Scolaro, A.D. Phillips, L. Lagopoulos, L. Juillerat- Jeanneret, G. Sava, R. Scopelliti, P.J. Dyson, J. Med. Chem. 50 (2007) 2166-2175;

(c) L.D. Dale, J.H. Tocher, T.M. Dyson, D.I. Edwards, D.A. Tocher, Anti-CancerDrug Des. 7 (1992) 3-14.

[15] (a) L.A. Huxham, E.L.S. Cheu, B.O. Patrick, B.R. James, Inorg. Chim. Acta. 352(2003) 238-246;

(b) Y.N.V. Gopal, D. Jayaraju, A.K. Kondapi, Biochemistry 38 (1999) 4382-4388.

[16] R.E. Morris, R.E. Aird, P.D.S. Murdoch, H. Chen, J. Cummings, N.D. Hughes, S. Parsons, A. Parkin, G. Boyd, D.I. Jodrell, P.J. Sadler, J. Med. Chem.44 (2001) 3616-3621.

[17](a) M.G. Mendoza-Ferri, C.G. Hartinger, R.E. Eichinger, N. Stolyarova, K. Severin, M.A. Jakupec, A.A. Nazarov, B.K. Keppler, Organometallics 27 (2008) 2405-2407;

(b) M.G. Mendoza-Ferri, C.G. Hartinger, A.A. Nazarov, W. Kandioller, K. Severin, B.K. Keppler, Appl. Organomet. Chem. 22 (2008) 326-332.

[18] B. Therrien, W.H. Ang, F. Cherioux, L. Vieille-Petit, L. Juillerat-Jeanneret, G. Suss-Fink, P.J. Dyson, J. Cluster Sci.18(2007) 741-752.

[19] C.S. Allardyce, P.J. Dyson, J. Cluster Sci.12 (2001) 563-569.

[20] R.K. Gupta, R. Pandey, G. Sharma, R. Prasad, B. Koch, S. Srikrishna, P.Z. Li, Q. Xu, D.S. Pandey, Inorg. Chem. 52 (2013) 3687-3698.

[21] S. Chatterjee, S. Kundu, A. Bhattacharyya, C.G. Hertinger, P.J. Dyson, J. Biol. Inorg. Chem. 13 (2008) 1149-1155.

[22] G. Gupta, A. Garci, B.S. Murray, P.J. Dyson, G. Fabre, P. Trouillas, F. Giannini, J. Furrer, G.Suss-Fink, B. Therrien, Dalton Trans. 42 (2013) 15457-15463.

[23] H.H. Monfared, M. Vahedpour, M.M. Yeganeh, M. Ghorbanloo, P. Mayer, C. Janiak, Dalton Trans. 40 (2011) 1286-1294.

[24] S. Patai, The Chemistry of Carbon–Nitrogen Double Bond, Interscience, New York, 1970.

[25] Y. Gou, Y.Zhang, J. Qi, Z. Zhou, F. Yang, H. Liang, J. Inorg. Biochem. 144 (2015) 47-55.

[26] P. Sathyadevi, P.Krishnamoorthy, R.R. Butorac, A.H. Cowley, N.S.P. Bhuvanesh and N. Dharmaraj, Dalton Trans. 40 (2011) 9690-9702.

[27] M.M. Dor-devic, D.A. Jeremic, M.V. Rodic, V.S. Simic, I.D. Brceski, V.M. Leovac, Polyhedron 68 (2014) 234-240.

[28] D.S. Raja, N.S.P. Bhuvanesh and K. Natarajan, Dalton Trans. 41 (2012) 4365-4377.

[29] W. Plass, A. Pohlmann, H.P. Yozgatli, J. Inorg. Biochem. 80 (2000) 181-183.

[30] R. Dinda, P. Sengupta, S. Ghosh, T.C.W. Mak, Inorg. Chem. 41 (2002) 1684-1688.

[31] M. Alagesan, P. Sathyadevi, P. Krishnamoorthy, N.S.P. Bhuvanesh and N. Dharmaraj, Dalton Trans. 43 (2014) 15829-15840.

[32] R.N. Prabhu, R. Ramesh, RSC Adv. 2 (2012) 4515-4524.

[33] R.J. Butcher, J. Jasinski, G.M. Mockler, E. Sinn, J. Chem. Soc. Dalton Trans. (1976) 1099-1102.

[34] N. Chitrapriya, V. Mahalingam, L.C. Channels, M. Zeller, F.R. Fronczek and K. Natarajan, Inorg. Chim. Acta. 361(2008) 2841-2850.

[35] S. Pal and S. Pal, Eur. J. Inorg. Chem. (2003) 4224-4252.

[36] A. Basu, T.G. Kasan and N.Y. Sapre, Inorg. Chem. 27 (1988) 4539-4546.

[37] M. Gras, B. Therrien, G.Suss-Fink, P. Stepnicka, A.K. Renfrew and P.J. Dyson J. Organometa. Chem. 693 (2008) 3419-3424.

[38] M. Auzias, B.Therrien, G. Suss-Fink, P. Stepnicka, W.H. Ang, P.J. Dyson, Inorg. Chem. 47 (2008) 578-583.

[39] A. Kurzwernhart, W. Kandioller, C. Bartel, S. Bachler, R. Trondl, G. Muhlgassner, M. A. Jakupec, V. B. Arion, D. Marko, B.K. Keppler and C.G. Hartinger, Chem. Commun. 48 (2012) 4839-4841.

[40] M.P. Chelopo, S.A. Pawar, M.K. Sokhela, T. Govender, H.G. Kruger, G.E.M. Maguire, Eur. J. Med. Chem. 66 (2013) 407-414.

[41] S.H. Kaufmann and M.O. Hengartner, Trends Cell Biol. 11 (2001) 526-534.

[42] (a) S.H. Kaufmann and W.C. Earnshaw, Exp. Cell Res. 256 (2000) 42-49;

(b) R. Yazdanparast, S. Bahramikia and A. Ardestani, Chem. Biol. Interact. 172 (2008) 176-184.

[43] D. Baskic, S. Popovic, P. Ristic and N.N. Arsenijevic, Cell Biol. Int. Rep. 30 (2006) 924-932.

[44] W.L.F. Armarego, C.L.L. Chai, Purification of Laboratory Chemicals, sixth ed. Butterworth-Heinemann, Oxford, UK, 2009, pp 69-79.

[45] M.A. Bennett, A.K. Smith, J. Chem. Soc. Dalton Trans. (1974) 233-241.

[46] F.H. Allen, W.D.S. Motherwell, P.R. Raithby, G.P. and R. Taylor, New. J. Chem. 23 (1999) 25-34.

[47] G.M. Sheldrick, ActaCrystallogr. Sect. A. 64 (2008)112-122.

- New (η^6-benzene) ruthenium(II) aroylhydrazone complexes have been synthesized
- X- ray analysis of the complex reveals a typical three leg piano stool structure
- Complexes are more potent against MCF-7 cells than cisplatin
- Fluorescence staining methods confirm apoptosis induced cell death